https://doi.org/10.5194/amt-2023-204
Preprint. Discussion started: 22 November 2023
© Author(s) 2023. CC BY 4.0 License.

Atmospheric Measurement Techniques Discussions

Multi-angle aerosol optical depth retrieval method based on improved surface reflectance

Lijuan Chen[1], Ren Wang[1], Ying Fei[2], Peng Fang[2],Yong Zha[2], Haishan Chen[1*]

[1]Key Laboratory of Meteorological Disaster, Ministry of Education (KLME)/Joint International Research Laboratory of Climate and Environment Change (ILCEC)/Collaborative Innovation Center on Forecast and Evaluation of Meteorological Disasters (CIC-FEMD), Nanjing University of Information Science and Technology, Nanjing 210044, China

[2]Key Laboratory of Virtual Geographic Environment of Ministry of Education, Jiangsu Center for Collaborative Innovation in Geographical Information Resource Development and Application, College of Geographic Science, Nanjing Normal University, Nanjing 210023, China

Correspondence: Haishan Chen (haishan@nuist.edu.cn)

Abstract

Retrieval of terrestrial aerosol optical depth (AOD) has been a challenge for satellite Earth observations, mainly due to the difficulty of estimating surface reflectance caused by land-atmosphere coupling. Current satellite AOD retrieval products have low spatial resolution under complex surface processes. In this study, based on our previous studies of AOD retrieval, we further improved the estimation method of surface reflectance by establishing an error correction model and then obtained a more accurate AOD. A lookup table is constructed using the Second Simulation of Satellite Signal in the Solar Spectrum (6S) to obtain high-precision retrieval of AOD. The retrieval accuracy of the algorithm is verified by AERONET (Aerosol Robotic Network) observations. The results indicate that the retrieved AOD based on the improved method

https://doi.org/10.5194/amt-2023-204
Preprint. Discussion started: 22 November 2023
© Author(s) 2023. CC BY 4.0 License.

Atmospheric Measurement Techniques Discussions

of this study has advantages in fewer missing AOD pixels and finer spatial resolution, as compared to the MODIS AOD product and our previous estimation method. Among the nine MISR angles, the optimal correlation coefficient (R) of retrieved AOD and observed AOD can reach 0.89. Root mean square error (RMSE) and relative mean bias (RMB) can reach a minimum values of 0.20 and 0.32, respectively. This study will help to further improve the accuracy of retrieving multi-angle AOD at large spatial scales and long time series.

Keywords: surface reflectance; aerosol optical depth; satellite remote sensing; MISR; MODIS

1. Introduction

Aerosols are liquid or solid particles suspended in the atmosphere, with particle diameters ranging from approximately 0.001 to 100 μm (Giles et al., 2019). Aerosols have a large impact on the Earth's radiation budget balance and the uncertainties are difficult to estimate (Holben et al., 2001; Li et al., 2020; Berhane et al., 2021; Sun et al., 2022), thus direct and indirect effects of aerosols have received widespread attention in the study of climate change mechanisms (Hatzianastassiou et al., 2009; Dao et al., 2014; Daniel et al., 2014; Samset et al., 2018; Li et al., 2018; Huang et al., 2021). In addition, concentrations of aerosols may pose a serious threat to human health (Lee et al., 2010; Dehghani et al., 2012; Mironova et al., 2015). The parameters of the optical properties of aerosols include aerosol optical depth (AOD), scattering phase function, single scattering albedo and absorbing optical depth, etc. As an important parameter, AOD is defined as the integral of aerosol extinction coefficient in the vertical direction. AOD describes the attenuation effect of aerosols on light and also reflects an important indicator of the degree of air pollution. Over the past two decades, multi-channel spectrometers carried by multiple

https://doi.org/10.5194/amt-2023-204
Preprint. Discussion started: 22 November 2023
© Author(s) 2023. CC BY 4.0 License.

Atmospheric Measurement Techniques Discussions

geostationary and polar orbit satellites have been used for AOD retrieval. The AOD products obtained from satellite retrieval are widely used in the study of atmospheric environment (Kaufman et al, 1997; Xie et al., 2019; Chen et al., 2021). Although the retrieval accuracy of AOD is constantly improving, there is still a lot of room for improvement in the retrieval results over land.

Scholars have conducted studies using multi angle sensors. Flowerdew et al. (1996) utilized Along Track Scanning Radiometer 2 (ATSR-2) dual angle observation data, based on the approximate condition of minimum variation of surface reflectance with wavelength, and using the assumption of independent invariance of ground features and Lambertian bodies, simulated using a bidirectional reflection radiation transfer model, and proposed a dual angle algorithm (ATSR-DV) to invert AOD over land. Kokhanovsky et al. (2009) used the ATSR-DV algorithm to invert the AOD over Germany on October 13, 2005, and compared the retrieval results with MEdium Resolution Imaging Spectrometer (MERIS) and MISR products, indicating that the ATSR-2 algorithm is also suitable for Advanced Along Track Scanning Radiometer (AATSR). Sundstrom et al. (2012) obtained an aerosol model of eastern China based on Aerosol Robotic Network (AERONET) observation data, and used the ATSR-DV algorithm to retrieve the proportion of AOD and coarse to fine particles from AATSR data. Abdou et al. (2005) compared the MISR AOD and the Moderate-resolution Imaging Spectroradiometer (MODIS) AOD products carried by Terra using data from 62 AERONET observation sites. The results showed that over land, the MODIS AOD in the 0.470 um and 0.660 um channels was 35% and 10% higher than MISR. In coastal and desert areas, the MODIS retrieval error was relatively large, while over the ocean, in the 0.470 um and 0.660 um channels, the MISR was 0.1 and 0.05 higher than the

https://doi.org/10.5194/amt-2023-204
Preprint. Discussion started: 22 November 2023
© Author(s) 2023. CC BY 4.0 License.

Atmospheric Measurement Techniques Discussions

MODIS AOD value, respectively, mainly depends on the accuracy of radiometric calibration. Martochik et al. (1997) proposed an algorithm for extracting aerosol optical parameters using MISR multi angle observations. The results showed that in the presence of dense vegetation over land, AOD was extracted using its low reflectivity and multi angle observations. If dense vegetation did not exist, AOD and aerosol models were determined using the reflectance function spectral contrast angle dependence relationship. As a new remote sensing tool, multi angle remote sensing has the ability to provide aerosol characteristics such as optical depth, single scattering albedo, and phase function with sufficient precision, which is more suitable for playing its unique role in aerosol research than traditional single angle optical remote sensing (Dubovik et al., 2019). Multi angle remote sensing retrieval of aerosol optical properties can utilize the angle information contained in satellite signals to better separate the contributions of the surface and atmosphere, making it suitable for some bright surfaces. This provides a new approach for AOD retrieval.

The surface reflectance measures the ability of land acquisition to absorb and reflect solar radiation. The surface reflectance is relatively complex on land, and its contribution is received by satellite detectors after atmospheric scattering and absorption. Satellite observations are obtained as a coupling of the two, making it difficult to directly distinguish between surface reflectance and atmospheric scattering. Therefore, simultaneous retrieval of atmospheric aerosols and surface reflectance is the goal pursued by quantitative satellite remote sensing (Deuzé et al., 2001). In optical remote sensing, the blue band has shorter wavelengths, relatively low surface reflectivity, and there is relatively more reflection and scattering caused by the atmosphere. Therefore, AOD is generally retrieved through the blue band. In the process of AOD retrieval, the overestimation of the surface reflectivity will lead to an underestimation of AOD, and the underestimation of surface

https://doi.org/10.5194/amt-2023-204
Preprint. Discussion started: 22 November 2023
© Author(s) 2023. CC BY 4.0 License.

Atmospheric Measurement Techniques Discussions

reflectance will lead to an overestimation of AOD. Separating atmospherically generated reflectance and surface reflectance from apparent reflectance is one of the difficulties of AOD retrieval (apparent reflectance is the reflectance at the top of the atmosphere). In general, signals such as aerosols are weaker compared to surface signals (Dong et al., 2023). Previous studies have shown that when using satellite remote sensing to retrieve AOD, an intercept error of 0.01 in surface reflectance can result in an retrieval error of approximately 0.1 (Zhang et al., 2021). Therefore, accurate estimates of surface reflectance are an important basis for aerosol retrieval.

A high-precision AOD product obtained from retrieval is of great significance for monitoring changes in atmospheric pollution and providing decision-making for pollution control. Observing the spatial distribution of AOD is very important for daily monitoring of air pollution. In addition, aerosol particles can affect the energy balance between the land and the atmosphere by absorbing and scattering solar radiation, thus affecting the global climate system. To further improve the retrieval accuracy and resolution of AOD, this study uses data from nine camera angles in the blue band of MISR L1B2T from 2016 to 2018 using an improved retrieval algorithm. Firstly, the study analyzes the retrieval errors of the MISR AOD for nine camera angles before the improved retrieval. Secondly, we established an error correction model to correct the estimated surface reflectance of MISR, thereby improving the surface reflectance at 9 angles. The improved surface reflectance retrieval is used to obtain the MISR AOD with high accuracy. Finally, the improved AOD retrieval method is verified and its estimated results are compared with the previous retrieval.

https://doi.org/10.5194/amt-2023-204
Preprint. Discussion started: 22 November 2023
© Author(s) 2023. CC BY 4.0 License.

Atmospheric Measurement Techniques Discussions

2. MISR, MODIS, and AERONET Data

2.1 MISR and MODIS data

The MISR sensor is manufactured by National Aeronautics and Space Administration (NASA) Jet Propulsion Laboratory (JPL) in the U.S. The MISR sensor consists of nine cameras, each fixed at a specific angle of view along the orbital direction.The MISR has four bands (Blue: 446 nm, Green: 558 nm, Red: 672 nm and Near InfraRed: 866 nm) and nine angle (Table S1). The MISR is capable of imaging the region almost simultaneously by all cameras within 7 min (Diner et al., 1998; Martonchik et al., 2002; Kahn et al., 2007). 36 channels of MISR data are included, all of which can be retrieved for AOD. Typically, medium angles are used for surface observations and large angles are more sensitive to the effects of cloud cover and atmospheric aerosols. The MISR product (MIL2ASAE_3) format is .nc, and the MISR format is HDF-EOS. The data used in this study are MISR Level 1B2 Terrain Projected Data (MI1B2T) data. The projection of the MI1B2T data is the Space Oblique Mercator (SOM), which uses Hierarchical Data Format - Earth Observing System (HDF-EOS) strip record data, and out of 233 paths, each of the 233 orbits consists of 180 mutually independent blocks (Kahn et al., 2005). The study extracted 64 and 65 blocks of data covering the Yangtze River Delta region (Fig. S1). MISR data cannot be directly processed using Arcgis and ENVI due to its special storage method. The study uses HDF-EOS To GeoTIFF Conversion Tool (HEGTool) for batch processing of MI1B2T and MI1B2GEOP. Using the HEGTool, the radiation data in the MI1B2T dataset is extracted, and as the radiation data contains 180 blocks, the corresponding blocks, output data types and projections are selected based on the area locations. Solar zenith angle, solar azimuth angle, satellite zenith angle for 9 cameras and satellite azimuth angle for 9 cameras data were extracted from the MI1B2GEOP, and

https://doi.org/10.5194/amt-2023-204
Preprint. Discussion started: 22 November 2023
© Author(s) 2023. CC BY 4.0 License.

Atmospheric Measurement Techniques Discussions

the corresponding blocks, output data types and projection information were selected. The TIFF data output by the software is only then available for the next step of processing using ARCGIS and ENVI. For the downloaded MISR data, remote sensing images with cloud pixels less than 50% are used for cloud detection and removal of cloud pixels. This study using blue bands to set thresholds to remove cloud pixels. After repeated experiments, if a fixed threshold is used, cloud pixels cannot be removed cleanly from the 9 observation angles of MISR (Fig. S2, Fig. S3). Therefore, this study uses dynamic threshold method to remove MISR cloud pixels from images. The dataset used in the study is shown in table S2.

MODIS L1B data are Earth observation data stored in a hierarchical (HDF) format , providing MOD02QKM, MOD02HKM and MOD021KM data respectively (Hong et al., 2007; Bandaru et al., 2013; Wong et al., 2020). MODIS geolocation data (MOD03/MYD03) contain the MODIS solar/satellite zenith angle for each 1 km EV (Earth View) centre, the latitude, longitude, solar/satellite azimuth and land/sea thresholds. To obtain the MODIS L1B apparent reflectance, MOD03/MYD03 solar zenith angle data are also used. The MODIS L1B data used for the study consisted of radiometric data (MOD02/MYD02) and geolocation data (MOD03/MYD03). The MODIS L1B data were pre-processed with the corresponding MOD03 data for geometric correction. The MODIS Conversion Toolkit (MCTK) was used to achieve radiometric calibration, "bowtie" processing, geometric correction, reprojection and band extraction of MODIS data. MODIS sensors can observe the surface at zenith angles up to approximately 65.5°, and repeated observations of the same surface image over multiple days can be obtained for different angles (-65.5° to 65.5°) of this image. Assuming that the surface of this image does not change significantly during this time, this set of multi-angle observations can be used for the BRDF

https://doi.org/10.5194/amt-2023-204
Preprint. Discussion started: 22 November 2023
© Author(s) 2023. CC BY 4.0 License.

Atmospheric Measurement Techniques Discussions

(Bidirectional Reflectance Distribution Function) model retrieval. MODIS BRDF/Albedo is a standard terrestrial level 3 product, generated from data acquired by the Terra and Aqua satellite platforms and MODIS. This product has a 16-day cycle, with observations on day 9 of the 16-day retrieval cycle being assigned a weight to obtain daily data, which is the global surface albedo daily product data (Hsu et al., 2004). The core dataset of the MODIS BRDF product is MCD43A1.

2.2 AERONET data

AERONET uses a French produced solar radiometer CE-318 instrument to obtain solar direct spectral radiation measurements at 340nm, 380nm, 440nm, 500nm, 670nm, 870nm, 936nm, 1020nm, and 1640nm channels every 3 minutes at a field of view angle of 1.5°. The total atmospheric water vapour content can be obtained from the 936 nm channel measurements and the AOD values can be retrieval using the remaining channel measurements with an retrieval error of about 0.01-0.02. Therefore, it can provide aerosol characterization parameters with high accuracy and validate the aerosol parameters from satellite retrievals (Lu et al., 2019). AERONET has more than 600 observing sites globally distributed over land and ocean, using a sun photometer as the basic observing instrument, and most of the sites achieve daily data acquisition and unified transmission to the network for centralized processing. It plays an important role in studying global aerosol radiation effects, aerosol transport, validating radiative transfer models and verifying satellite remote sensing aerosol results. The study therefore examines the accuracy of the satellite remote sensing retrieval of AOD using the AOD measured by AERONET as the true value.

AERONET provides observations of AOD, retrieval products and precipitable water

https://doi.org/10.5194/amt-2023-204
Preprint. Discussion started: 22 November 2023
© Author(s) 2023. CC BY 4.0 License.

Atmospheric Measurement Techniques Discussions

distributed over a wide range of aerosol patterns worldwide. There are three quality levels of AOD data. Level 1.0 (unscreened), Level 1.5 (cloud-screened and quality-controlled), and Level 2.0 (quality-assured). The study area is mainly the Yangtze River Delta region of China, where AERONET has a large number of sites, but only the Taihu and Xuzhou-CUMT sites provide continuous data, while the rest of the sites have been acquiring data for a relatively short period of time.

The amount of available data for AERONET AOD Level 2 is relatively small. To ensure sufficient ground site validation data, this study selected Level 1.5 data with a large and continuous amount of current observation data to verify the satellite remote sensing AOD obtained from retrieval (Dubovik et al., 2000; Li et al., 2009) . In terms of time, the AERONET AOD Level 1.5 data selected for this study correspond to the MISR data for the three years from 2016-2018, respectively.

3. Methodology

3.1 Problems in the previous surface reflectance estimation method

Accurate estimation of the contribution of surface reflectance has been the focus and difficulty in the process of remote sensing retrieval of AOD (Remer et al., 2009; Gupta et al., 2016). Previous study used MODIS BRDF data and MODIS V5.2 Algorithm to determine the MODIS surface reflectance (Chen et al., 2021), and after spectral conversion between the two sensors, MODIS and MISR, the MISR surface reflectance was obtained for nine angles. A look-up table was constructed using the Second Simulation of Satellite Signal in the Solar Spectrum (6S), and then the MISR surface reflectance of the 9 angles was combined to obtain the MISR AOD of

https://doi.org/10.5194/amt-2023-204
Preprint. Discussion started: 22 November 2023
© Author(s) 2023. CC BY 4.0 License.

Atmospheric Measurement Techniques Discussions

different angles by retrieval. This study found the variation pattern of the MISR AOD of the 9 angles. However, the error of the 9-angle retrieved MISR AOD was relatively large compared to the AERONET AOD (Table S3).

In 6S model, a series of parameters related to the simulated imaging date atmospheric conditions need to be input, including geometric parameters, AOD, water vapor, ozone, elevation, etc. At the same time, these parameters are inputted through a simple and intuitive lookup table. Finally, a linear atmospheric correction formula is generated to obtain the surface reflectance values after 6S atmospheric correction for each pixel in each band one by one. The 6S model inputs the geometric parameter information corresponding to the MISR image at the the Taihu and Xuzhou-CUMT sites, and the input of 550nm AOD parameters is the AERONET AOD of the two sites. Then, the 6S model is used to obtain the MISR atmospheric corrected reflectance. To analyze the overall high AOD values retrieved from 9 angles of MISR, this study compared the MISR atmospheric corrected reflectance at that pixel position with the MISR surface reflectance (Fig. 1) (The calculation method for MISR surface reflectance refers to chen et al. (2021)). It can be seen that the MISR surface reflectance is low compared to the value of MISR atmospheric corrected reflectance at the corresponding locations of the two sites, resulting in a higher retrieve MISR AOD compared to the AERONET AOD. Therefore, it is necessary to establish a correction model to correct the MISR surface reflectance to improve the retrieval accuracy of the MISR AOD.

https://doi.org/10.5194/amt-2023-204
Preprint. Discussion started: 22 November 2023
© Author(s) 2023. CC BY 4.0 License.

Atmospheric Measurement Techniques Discussions

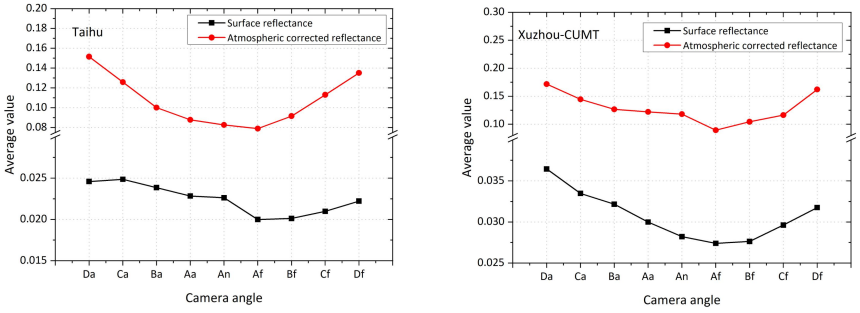

214 Figure 1. Comparison of MISR surface reflectance with atmospheric corrected reflectance in the
215 blue band (At the pixel locations of Taihu and Xuzhou-CUMT sites).

216 **3.2 Improved surface reflectance estimation method**

217 In order to develop a correction model to improve the surface reflectance, the design scheme
218 of this study is shown below:

219 a) Atmospheric correction of MODIS L1B using the 6S model to obtain MODIS atmospheric
220 corrected reflectance;

221 b) The new estimated MISR surface reflectance based on the MODIS atmospheric correction
222 was calculated by bringing the MODIS atmospheric correction reflectance into Eq. 1 and Eq. 2.
223 The MISR surface reflectance was combined with the newly estimated MISR surface reflectance
224 and a regression was fitted (with 60% of the overall sample data randomly selected) to create a
225 surface reflectance error correction model, as shown in the following formula:

226
$$\rho(\theta_s,\theta_v,\phi)_{MISR\_a} = \rho(\theta_s,\theta_v,\phi)_{MODIS\_at} \times \frac{BRDF(\theta_s,\theta_v,\phi)_{MISR}}{BRDF(\theta_s,\theta_v,\phi)_{MODIS}} \quad (1)$$

227 In Eq. (1), $BRDF(\theta_s,\theta_v,\phi)_{MISR}$, $BRDF(\theta_s,\theta_v,\phi)_{MODIS}$ are BRDFs obtained at MISR and
228 MODIS angles, respectively. θ_s is the solar zenith angle, θ_v is the satellite zenith angle, and ϕ is
229 the relative azimuth angle. $\rho(\theta_s,\theta_v,\phi)_{MISR\_a}$ is the surface reflectance of MODIS at the

https://doi.org/10.5194/amt-2023-204
Preprint. Discussion started: 22 November 2023
© Author(s) 2023. CC BY 4.0 License.

Atmospheric Measurement Techniques Discussions

geometric observation angle of MISR, and $\rho(\theta_s,\theta_v,\phi)_{MODIS\_at}$ is the MODIS atmospheric corrected reflectance.

This study selected spectral data containing 28 typical features of different types of vegetation, soil and water bodies from five standard spectral libraries that come with the ENVI software. Calculate the surface reflectance of different features in the blue bands of MODIS and MISR using formulas (Chen et al., 2021).

$$\rho(\theta_s,\theta_v,\phi)_{MISR} = \rho(\theta_s,\theta_v,\phi)_{MISR\_a} \times 0.9834 - 0.0081 \quad (2)$$

The New MODIS surface reflectance ($\rho(\theta_s,\theta_v,\phi)_{MISR\_a}$) at the MISR angle obtained from Eq. (1) is converted to the MISR surface reflectance by Eq. (2).

c) The MISR surface reflectance estimated by Eq. 2 is transformed by an error correction model to obtain the final improved MISR surface reflectance. The improved MISR surface reflectance will be used in the retrieval of the AOD. The MISR correction model was developed by fitting a linear regression of the previously estimated MISR surface reflectance based on the MODIS V5.2 algorithm to the MISR surface reflectance estimated based on the MODIS atmospheric correction (60% of the data were randomly selected) as shown in Eq. 3. The previously estimated 9-angle MISR surface reflectance was error-corrected by Eq. 3 to obtain the improved surface reflectance for the 9 angles of the MISR sensor, which was ultimately used to perform the MISR AOD retrieval for the 9 angles.

$$\rho(\theta_s,\theta_v,\phi)_{MISR-b}{}^{*} = \rho(\theta_s,\theta_v,\phi)_{MISR} \times 0.9209 + 0.0409 \quad (3)$$

Where $\rho_{MISR-b}{}^{*}$ is the improved MISR surface reflectance in Eq. (3).

https://doi.org/10.5194/amt-2023-204
Preprint. Discussion started: 22 November 2023
© Author(s) 2023. CC BY 4.0 License.

Atmospheric Measurement Techniques Discussions

3.3 Flow of improved multi-angle AOD retrieval

The flow of the improved surface reflectance algorithm for this study is shown in Fig. 2. The MODISL1B data were first atmospherically corrected using 6S, and then the MISR surface reflectance estimated from previous study was combined with the new MISR surface reflectance estimated from Eq. 2 to build a MISR error correction model to obtain the improved MISR surface reflectance (Chen et al., 2021). The study retrieved the MISR AOD for nine camera angles using improved MISR surface reflectance. We use AERONET AOD to validate the improved MISR AOD. Compare the improved AOD with the previously retrieved AOD, and analyze the accuracy and spatial distribution trend of the improved AOD. The AOD retrieval method used in this study is based on chen et al. (2021). The selection of appropriate aerosol type is very critical for the retrieval of aerosol optical depth. It has been shown that continental aerosols can be used for AOD retrieval in the Yangtze River Delta (He et al., 2015). Therefore, we used continental aerosols in our aerosol retrieval for the study area.

https://doi.org/10.5194/amt-2023-204
Preprint. Discussion started: 22 November 2023
© Author(s) 2023. CC BY 4.0 License.

Atmospheric Measurement Techniques Discussions

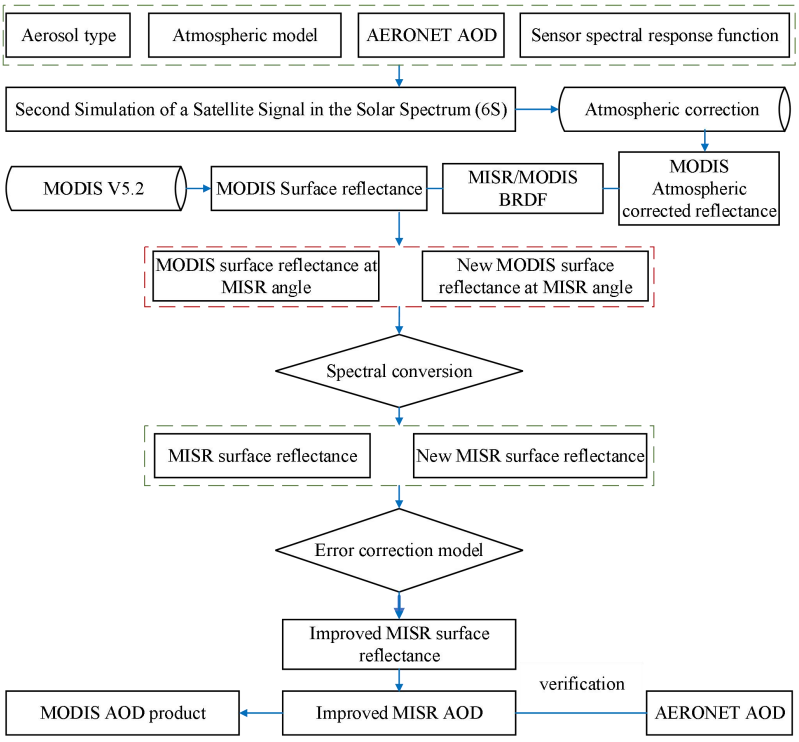

Figure 2. Flow chart of the improved MISR surface reflectance algorithm

4. Results and discussion

4.1 Improved MISR surface reflectance variation characteristics

The estimated MISR surface reflectance, the MISR atmospheric corrected reflectance and the improved MISR surface reflectance are presented in the Fig. 3. This is the average of all sample data at the corresponding locations at the two sites in Taihu and Xuzhou-CUMT for the valid dates of 2016-2018. It can be noted that at the two site of Taihu and Xuzhou-CUMT, the 9 camera angle MISR-improved surface reflectance values are overall higher than the MISR surface reflectance and lower than the MISR atmospheric corrected reflectance. The nine camera angle MISR surface reflectance values ranged from 0.02 to 0.04. The improved surface reflectance averages were

https://doi.org/10.5194/amt-2023-204
Preprint. Discussion started: 22 November 2023
© Author(s) 2023. CC BY 4.0 License.

Atmospheric Measurement Techniques Discussions

overall greater than the previously estimated MISR surface reflectance.

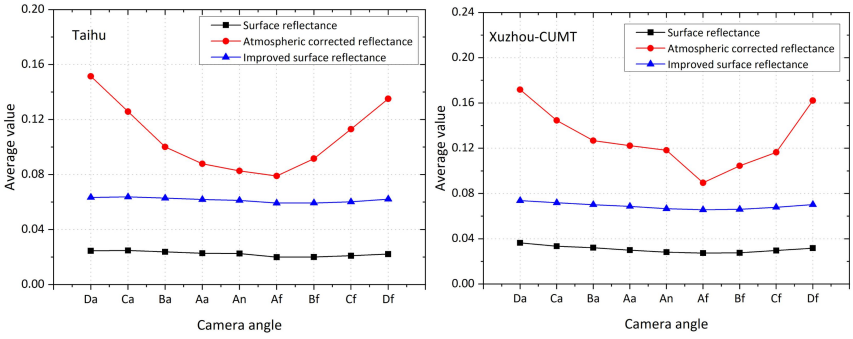

Figure 3. Comparison of MISR surface reflectance, atmospheric corrected reflectance and improved surface reflectance in the blue band (This is the multi-year average of the sample data for the two sites in Taihu and Xuzhou-CUMT).

To clarify the trend of the improved surface reflectance, the study performed a time-series analysis of the MISR surface reflectance and the improved surface reflectance (Fig. 4). It can be seen that the improved MISR surface reflectances are all higher than the previously estimated MISR surface reflectances. MISR surface reflectance values generally range from 0-0.05, with improved surface reflectance values ranging from approximately 0.05-0.1. The improved surface reflectance values have increased overall.

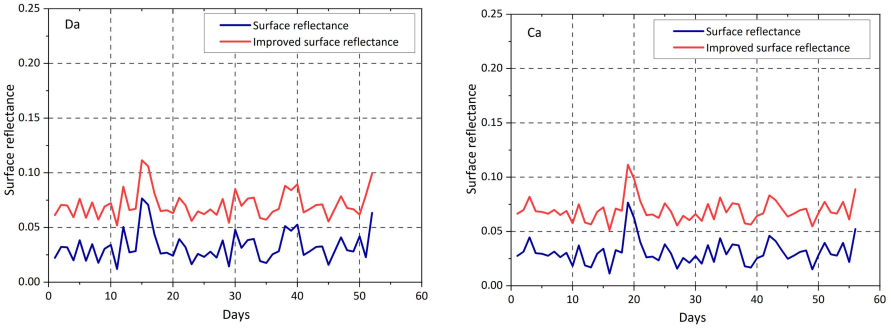

https://doi.org/10.5194/amt-2023-204
Preprint. Discussion started: 22 November 2023
© Author(s) 2023. CC BY 4.0 License.

Atmospheric Measurement Techniques Discussions

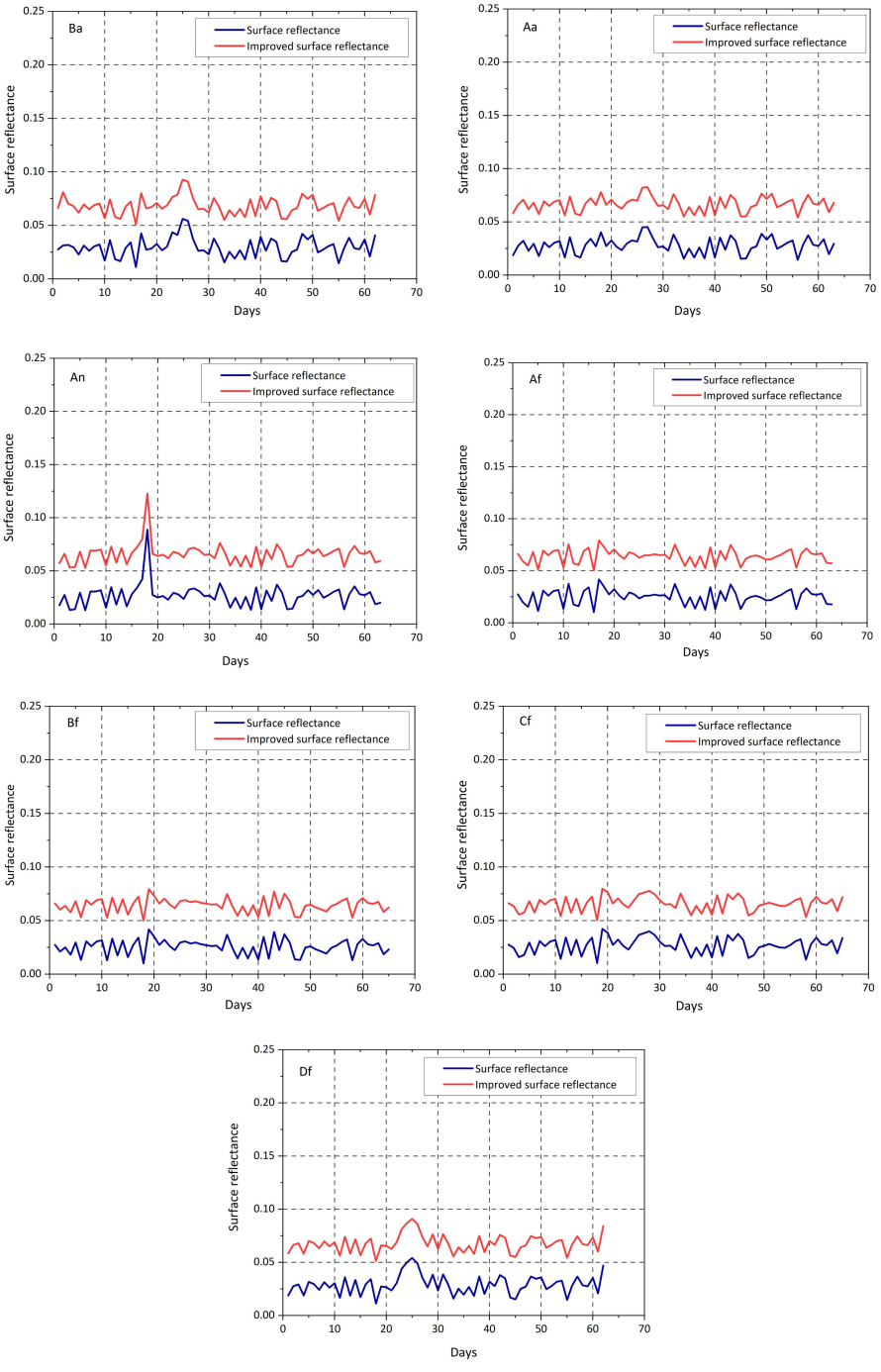

284 **Figure 4.** Surface reflectance time series of MISR sensors in the blue band at 9 observation angles.

285 (The order of time from front to back for 9 angles is shown in Table S2)

https://doi.org/10.5194/amt-2023-204
Preprint. Discussion started: 22 November 2023
© Author(s) 2023. CC BY 4.0 License.

Atmospheric Measurement Techniques Discussions

4.2 Results of the Improved MISR AOD retrieval

MISR AOD for 2016-2018 were obtained using an improved surface reflectance retrieval. The study presents retrieval results from nine camera observation angles of the MISR sensor on 12 June 2018 (Fig. 5). As can be seen from the spatial distribution of AOD, the retrieval results in the study area do not exceed a value of 1. The overall spatial distribution trend is generally consistent with the results before the improvement (Chen et al., 2021), but differs in the magnitude of the values. Values in the north-eastern and southern regions range from 0.5 to 1, indicating to some extent that the air quality in this region is poor. The five camera observation angles, Ba, Aa, An, Af and Bf, retrieve AOD values in the approximate range of 0.25-0.5. In the central region, the four camera observation angle values of Da, Ca, Cf and Df were mostly in the range of 0-0.25. The values indicate that the air quality in the region is generally good, but there are some areas of light air pollution. The higher AOD in the southern part of Shandong Province and the northern part of Jiangsu Province may be due to increased local aerosol emissions caused by human activities.

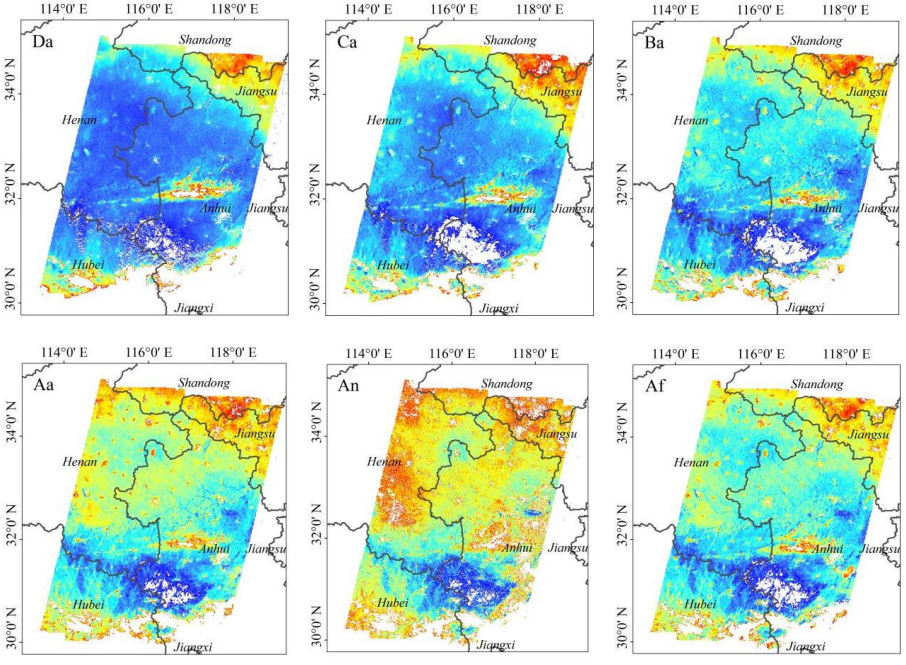

https://doi.org/10.5194/amt-2023-204
Preprint. Discussion started: 22 November 2023
© Author(s) 2023. CC BY 4.0 License.

Atmospheric Measurement Techniques Discussions

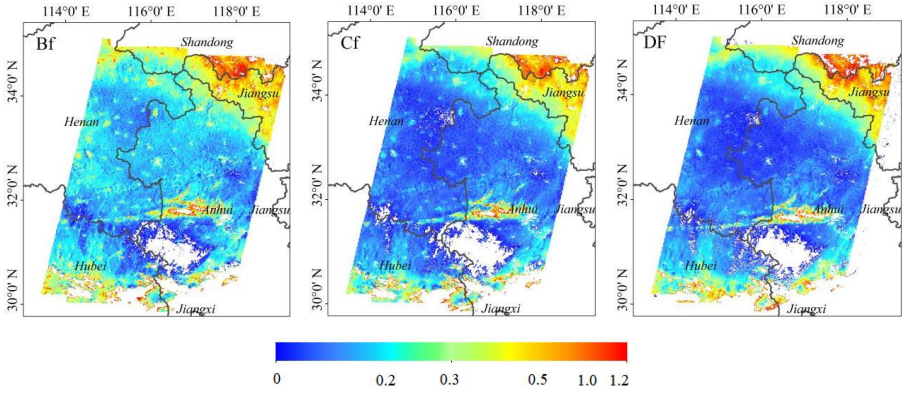

300 **Figure 5.** Plot of AOD 550nm retrieval results for the improved MISR 9 camera angles on 12
301 June 2018.

302 The study validates our improved MISR AOD spatial distribution results by comparing with
303 MODIS AOD products of the same date (Fig. 6). The MODIS AOD products have a resolution of
304 3km. It can be seen that the trend of spatial distribution of MODIS AOD products is consistent
305 with the improved MISR AOD. However, the MODIS AOD product has more missing data,
306 which can be avoided by the AOD obtained from the retrieval of the improved algorithm, and the
307 AOD retrieval by the improved algorithm has a higher resolution by comparing with the image
308 quality of the MISR AOD product.

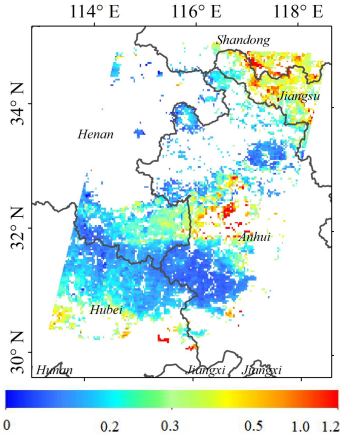

309 **Figure 6**. MODIS AOD 550nm product spatial distribution on June 12, 2018

https://doi.org/10.5194/amt-2023-204
Preprint. Discussion started: 22 November 2023
© Author(s) 2023. CC BY 4.0 License.

Atmospheric Measurement Techniques Discussions

4.3 Verification of the improved MISR AOD

There are many AERONET sites in the Yangtze River Delta region, but so far, only the Taihu and Xuzhou-CUMT sites continue to provide data, and other sites have a short time to obtain data. Therefore, the Taihu and Xuzhou-CUMT sites with more data are selected for verification. To verify the retrieved MISR AOD, In terms of time, we selected effective AOD records in the 550 nm band within a 30 minute interval between the AERONET ground observation site and the Terra satellite. The 9 camera views of MISR require about 7 minutes to observe the same geographical location, with relatively short intervals. Therefore, we will use the calculated AERONET AOD average as the approximate truth value, and compare the average value with the retrieved MISR AOD to verify and reduce errors caused by time difference. In terms of space, we selected pixels observed by MISR sensors from 9 angles and compared them with the nearest data observed by AERONET, which can reduce errors caused by spatial differences. The solar photometer does not have a 550 nm wavelength that corresponds to the retrieval results, and the AOD at 550 nm can be calculated by applying Angstrom (Eq. 4).

$$\tau(\lambda) = \beta\lambda^{-\alpha} \tag{4}$$

In the formula, $\tau(\lambda)$ is the AOD at wavelength λ, β is the concentration of the entire atmospheric aerosol, and α is the wavelength index of Angstrom.

In this study, four parameters will be used to assess the accuracy of the remotely sensed AOD dataset, namely the correlation coefficient (R), the Root Mean Square Error (RMSE), p-value and the relative mean bias (RMB). The specific calculation principles for the three parameters R, RMSE and RMB are shown in Eq. (5)-(7). The validation results of this study's improved AOD dataset from 2016-2018 at Taihu and Xuzhou-CUMT sites are shown in Fig. 7 and Fig. 8.

In general, the scatter plot is distributed above and below the 1:1 line. R is a parameter used to characterize the correlation between the remote sensing retrieval results and the ground-based retrieval results. At the Taihu site, R reach up to 0.89. At the Xuzhou-CUMT site, R reach up to 0.85. The RMSE is a parameter used to characterise the absolute error of the remote sensing retrieval results, with a minimum root mean square error of 0.21 at the Taihu site and 0.20 at the

https://doi.org/10.5194/amt-2023-204
Preprint. Discussion started: 22 November 2023
© Author(s) 2023. CC BY 4.0 License.

Atmospheric Measurement Techniques Discussions

Xuzhou-CUMT site. RMB is the parameter used to characterise the relative error of the remote sensing retrieval results, with a minimum RMB of 0.52 at the Taihu site and 0.32 at the Xuzhou-CUMT site. In summary, by comparing the results with the validation of the AOD scatter plot before the improvement, the accuracy of the nine camera observation angles at both sites has improved after the improvement (Table 1).

$$R = \frac{\sum_{i=1}^{N}(A_i - \overline{A})(A_i^{'} - \overline{A^{'}})}{\sqrt{\sum_{i=1}^{N}(A_i - \overline{A})^2 \sum_{i=1}^{N}(A_i^{'} - \overline{A^{'}})^2}} \quad (5)$$

$$RMSE = \sqrt{\sum_{i=1}^{N}(A_i - A_i^{'})^2 / N} \quad (6)$$

$$RMB = \sum_{i=1}^{N}(A_i - A_i^{'}) / N \quad (7)$$

where A_i is the retrieve MISR AOD, $A_i^{'}$ is the corresponding AERONET AOD, $\overline{A}$ and $\overline{A^{'}}$ are the mean values of the retrieve MISR AOD and AERONET AOD, respectively. N is the number of valid matching results for AERONET AOD and MISR AOD.

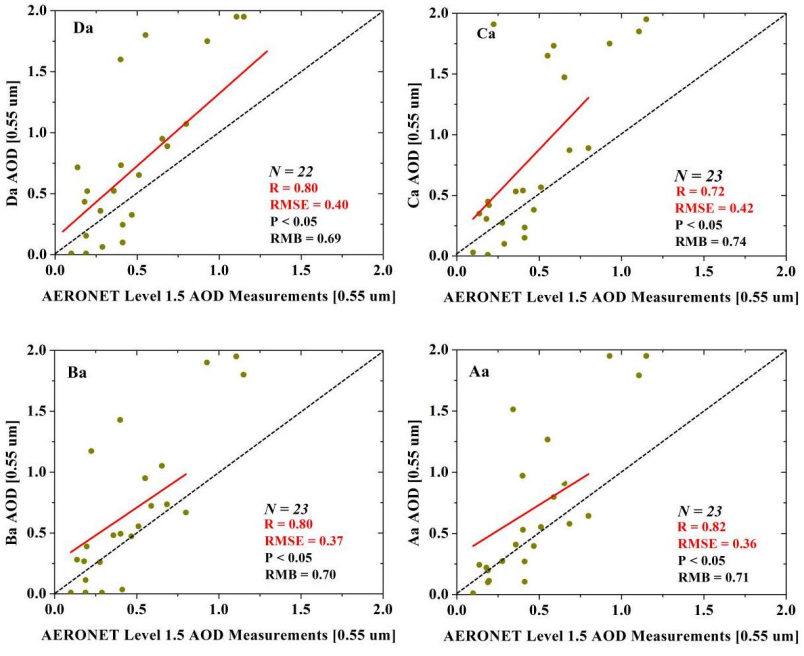

https://doi.org/10.5194/amt-2023-204
Preprint. Discussion started: 22 November 2023
© Author(s) 2023. CC BY 4.0 License.

Atmospheric Measurement Techniques Discussions

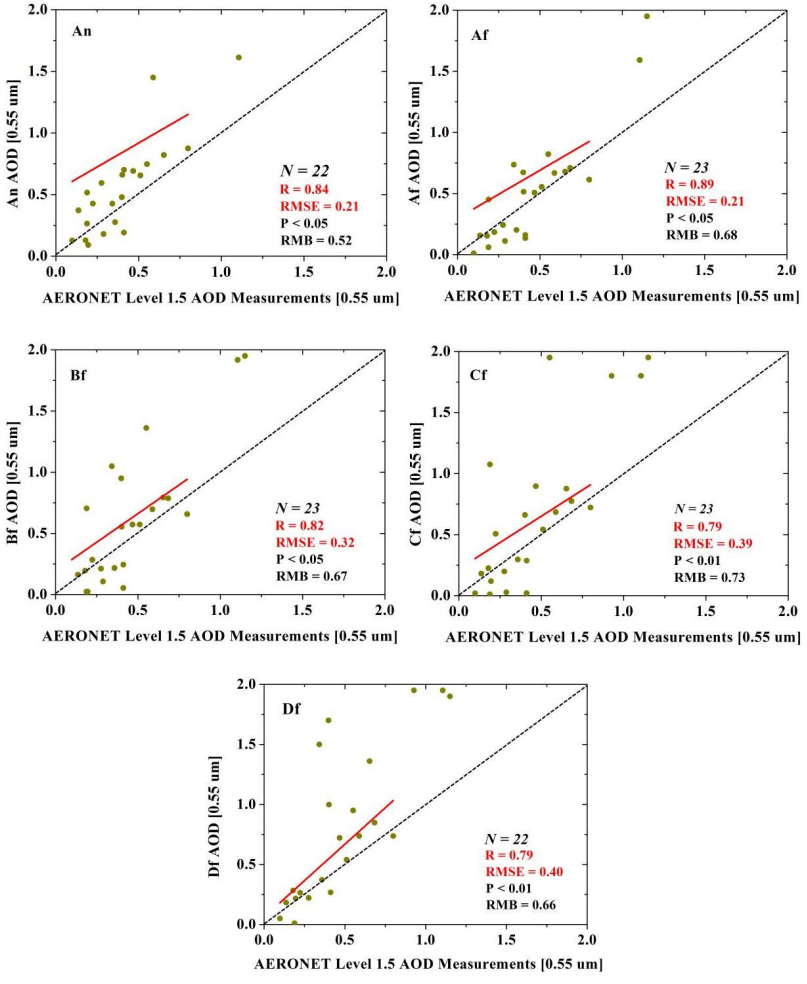

348 **Figure 7.** Comparison between improved MISR AOD and AERONET AOD at Taihu site (N is
349 the number of verification points, red line represents a linear fitting line).

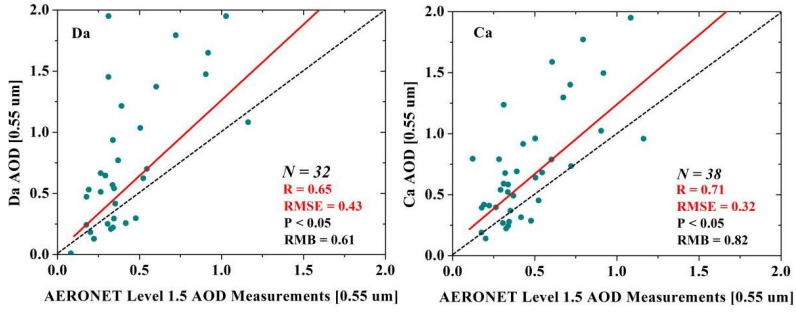

https://doi.org/10.5194/amt-2023-204
Preprint. Discussion started: 22 November 2023
© Author(s) 2023. CC BY 4.0 License.

Atmospheric Measurement Techniques Discussions

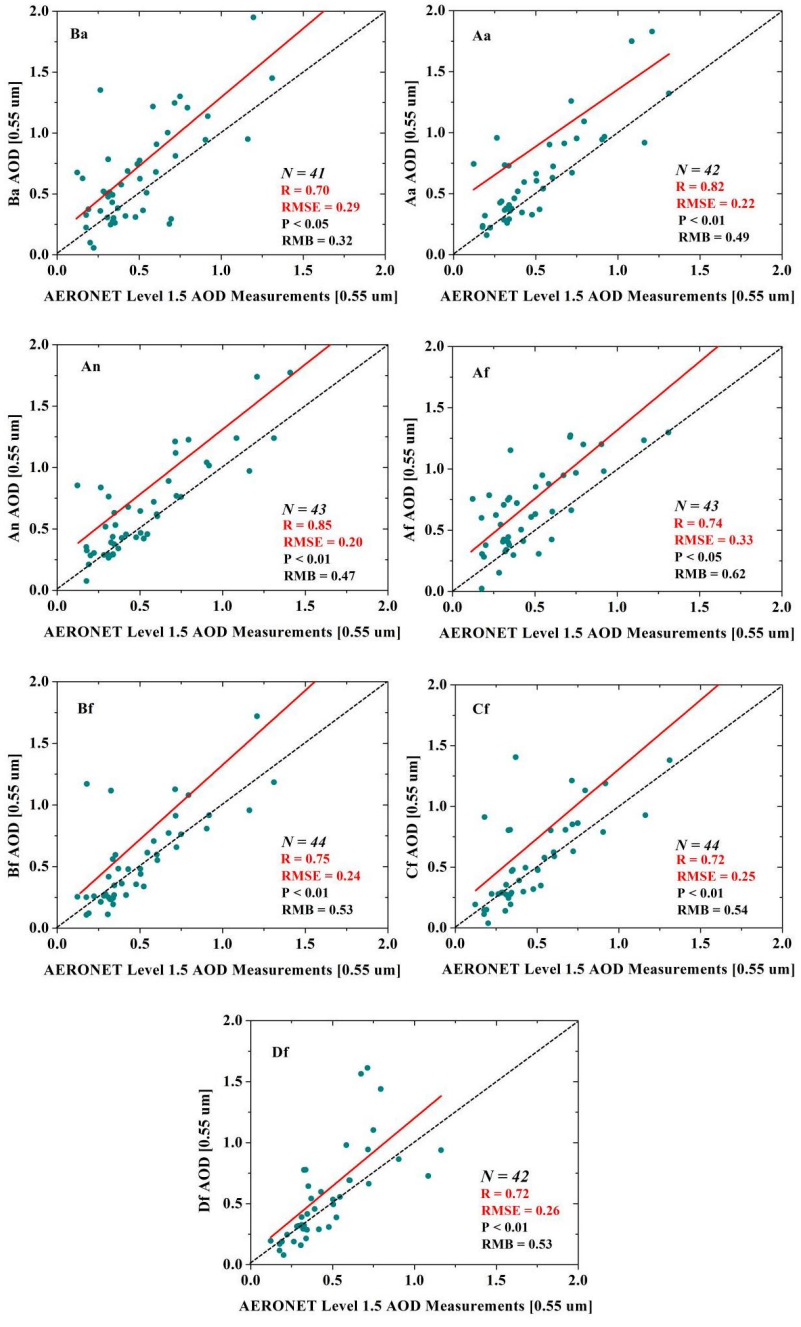

350 **Figure 8.** Comparison between improved MISR AOD and AERONET AOD at Xuzhou-CUMT

351 site (N is the number of verification points, red line represents a linear fitting line).

https://doi.org/10.5194/amt-2023-204
Preprint. Discussion started: 22 November 2023
© Author(s) 2023. CC BY 4.0 License.

Atmospheric Measurement Techniques Discussions

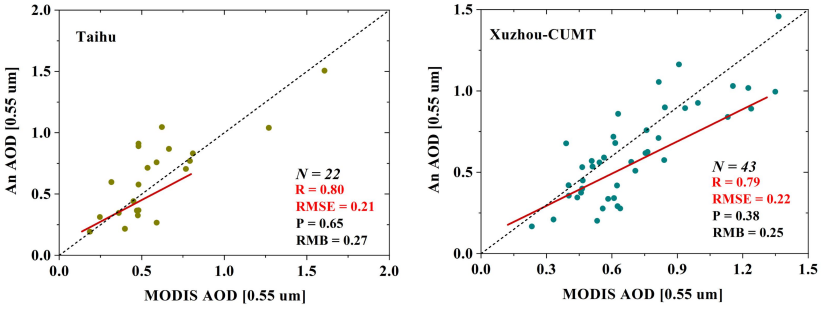

352 **Figure 9.** Comparison of validation of retrieved AOD with MODIS AOD product

353 **Table 1.** Precision comparison of MISR AOD and AERONET AOD before

354 and after improvement

Site	Angle	R	RMSE	RMB	Improved R	Improved RMSE	Improved RMB
Taihu	Da	0.77	0.20	1.08	0.80	0.40	0.69
	Ca	0.70	0.29	1.00	0.72	0.42	0.74
	Ba	0.77	0.14	0.61	0.80	0.37	0.70
	Aa	0.81	0.11	0.68	0.82	0.36	0.71
	An	0.45	0.29	1.22	0.84	0.21	0.52
	Af	0.72	0.14	0.87	0.89	0.21	0.68
	Bf	0.72	0.17	0.60	0.82	0.32	0.67
	Cf	0.57	0.24	0.65	0.79	0.39	0.73
	Df	0.77	0.20	0.47	0.79	0.40	0.66
Xuzhou-CUMT	Da	0.45	0.36	1.58	0.65	0.43	0.61
	Ca	0.59	0.34	0.96	0.71	0.32	0.82
	Ba	0.67	0.27	0.78	0.70	0.29	0.32
	Aa	0.73	0.24	0.78	0.82	0.22	0.49
	An	0.75	0.20	0.85	0.85	0.20	0.47
	Af	0.72	0.23	0.63	0.74	0.33	0.62
	Bf	0.62	0.28	0.65	0.75	0.24	0.53
	Cf	0.68	0.28	0.66	0.72	0.25	0.54
	Df	0.67	0.30	0.65	0.72	0.26	0.53

355

356 By comparing the validation results of MODIS AOD products with those of observation sites

357 (Taihu: R=0.59, RMSE=0.19, P<0.05, RMB=0.52; Xuzhou-CUMT: R=0.71, RMSE=0.25, P<0.05,

358 RMB=0.44) (Chen et al., 2021), we find that the improved MISR AOD has a higher correlation

https://doi.org/10.5194/amt-2023-204
Preprint. Discussion started: 22 November 2023
© Author(s) 2023. CC BY 4.0 License.

Atmospheric Measurement Techniques Discussions

with MODIS AOD products in the Taihu and Xuzhou-CUMT sites. The smaller the observation angle of the improved MISR AOD, the closer the error is to that of the MODIS AOD product. The observation angle of MISR An is the same as that of MODIS. Therefore, we selected An observation angle and MODIS AOD products at two pixel positions in the Taihu and Xuzhou-CUMT for verification (Fig. 9). The results show that the An AOD retrieval by the improved algorithm correlates well with the MODIS AOD product, and the position errors of the two image elements are close to each other. The RMSE of Xuzhou-CUMT site is slightly higher than that of Taihu site, and the RMB of Taihu site is slightly higher than that of Xuzhou-CUMT site.

5. Conclusion

This study first explored the problem of estimating the surface reflectance in our previous study and then obtained an error correction model for the surface reflectance using a linear fit of the MISR surface reflectance and a new estimate of the MISR surface reflectance. The improved MISR surface reflectance was obtained by means of an error correction model. A new AOD product was retrieved using the improved surface reflectance and a look-up table constructed from 6S model. Two AERONET ground observation sites with longer time series were used to validate the AOD obtained by satellites.

(1) Overall, the improved AOD and its spatial distribution trends are consistent with our previous results. The AOD estimated by our improved method presented a higher accuracy and a high degree of agreement with the AERONET ground-based observational AOD.

(2) More importantly, compared to the MODIS AOD products, the retrieved AOD in this study has fewer missing AOD pixels and finer spatial resolution. The retrievals of An Angle AOD by the improved algorithm are highly correlated with the MODIS AOD products, as shown through validation with the MODIS AOD product.

https://doi.org/10.5194/amt-2023-204
Preprint. Discussion started: 22 November 2023
© Author(s) 2023. CC BY 4.0 License.

Atmospheric Measurement Techniques Discussions

(3) In the future, more aerosol models conforming to the actual situation in the study area can be constructed using the AERONET ground observation data and introduced into the MISR AOD retrieval algorithm to further improve the accuracy of the AOD retrieval results. In this study, the AERONET AOD was used as the true value and as an input to the AOD parameter in the 6S model for atmospheric correction of MISR and MODIS images. A surface reflectivity error correction model was then obtained to retrieve the AOD for the entire region. It should be emphasized that the more AERONET sites used to train the corrected model, the more accurate the AOD results obtained by this method. However, the data of AERONET ground observation sites was limited. In the future, the study area can be expanded to large scale and longer time series.

Acknowledgement

This study was supported by the Key Program of the National Natural Science Foundation of China (42130609), Jiangsu Funding Program for Excellent Postdoctoral Talent (2023ZB482), the Natural Science Foundation of Jiangsu Province of China (BK20220455), and the National Science Foundation of China (42201028).

Competing interests

The contact author has declared that none of the authors has any competing interests.

https://doi.org/10.5194/amt-2023-204
Preprint. Discussion started: 22 November 2023
© Author(s) 2023. CC BY 4.0 License.

Atmospheric Measurement Techniques Discussions

Reference

Abdou, W. A.; Diner, D. J.; Martonchik J. V.; Bruegge C. J. Comparison of coincident Multiangle Imaging Spectroradiometer and Moderate Resolution Imaging Spectroradiometer aerosol optical depths over land and ocean scenes containing Aerosol Robotic Network sites. J. Geophys Res-atmos. 2005, 110 (D10): 1-12.

Bandaru, V.; West, T. O.; Ricciuto, D. M.; Izaurralde, R. C. Estimating crop net primary production using national inventory data and modis-derived parameters. Isprs. J Photogramm. 2013, 80, 61-71.

Berhane, S. A.; Bu, L. Aerosol-Cloud Interaction with Summer Precipitation over Major Cities in Eritrea[J]. Remote Sens-basel, 2021, 13(4):21.

Chen, L.; Wang, R.; Han J. Influence of observation angle change on satellite retrieval of aerosol optical depth[J]. Tellus B, 2021, 73.

Chen, L.; Fei, Y.; Wang, R. Retrieval of high temporal resolution aerosol optical depth using the GOCI remote sensing data[J]. Remote Sens-basel. 2021, 13:2376.

Chen, L.; Wang, R.; Wei, G. A surface reflectance correction model to improve the retrieval of MISR aerosol optical depth supported by MODIS data[J]. Adv Space Res, 2021, 67(2):858-867.

Dao, Y.; Gong, W. Observed holiday aerosol reduction and temperature cooling over East Asia[J]. J Geophys Res-atmos, 2014.

Daniel, R.; Steven, S.; Robert, W.; Leo, D. Climate Effects of Aerosol-Cloud Interactions[J]. Science, 2014, 343, 379-380.

Dehghani, M.; Saeedi, A. A.; Zamanian, Z. A study of the relationship between indoor and outdoor particle concentrations in Hafez hospital in Shiraz[J]. Phys.Rev.C, 2012.

Diner, D. J.; Beckert, J. C.; Reilly, T. H.; Bruegge, C. J.; Conel, J. E. Multi-angle imaging SpectroRadiometer (MISR) instrument description and experiment overview. IEEE Trans. Geosci. Remote Sens. 1998, 36, 1072–1087.

Dong, W.; Tao, M.; Xu, X.; Wang, J.; Wang, Y.; Wang, L.; Song, Y.; Fan, M.; Chen, L. Satellite

https://doi.org/10.5194/amt-2023-204
Preprint. Discussion started: 22 November 2023
© Author(s) 2023. CC BY 4.0 License.

Atmospheric Measurement Techniques Discussions

427 Aerosol Retrieval From Multiangle Polarimetric Measurements: Information Content and
428 Uncertainty Analysis," IEEE Trans. Geosci. Remote Sens. 2023, 61, 1-13.
429 Dubovik, O.; Smirnov, A.; Holben, B. Accuracy assessments of aerosol optical properties retrieved
430 from Aerosol Robotic Network (AERONET) Sun and sky radiance measurements[J]. J
431 Geophys Res-atmos, 2000, 105(D8): 9791-9806.
432 Dubovik, O.; Li.; Mishchenko M. I. Polarimetric remote sensing of atmospheric aerosols:
433 Instruments, methodologies, results, and perspectives[J]. Pergamon, 2019, 474-511.
434 Deuzé, J. L.; Bréon, F. M.; Devaux, C.; Goloub, P.; Herman, M.; Lafrance, B.; Maignan, F.;
435 Marchand, A.; Nadal, F.; Perry, G.; Tanré, D. Remote sensing of aerosols over land surfaces
436 from POLDER-ADEOS-1 polarized measurements. J Geophys Res-atmos, 2001, 106(D5):
437 4913-4926.
438 Flowerdew, R. J.; Haigh, J. D. Retrieval of aerosol optical thickness over land using the ATSR-2
439 Dual-look Satellite Radiometer. Geophys Res. Lett. 1996, 23 (4): 351-354.
440 Giles, D. M.; Sinyuk, A.; Sorokin, M. G. Advancements in the Aerosol Robotic Network
441 (AERONET) Version 3 database-automated near-real-time quality control algorithm with
442 improved cloud screening for Sun photometer aerosol optical depth (AOD) measurements[J].
443 Copernicus GmbH, 2019, 12(1), 169-209.
444 Gupta, P.; Levy, R. C.; Mattoo, S. A surface reflectance scheme for retrieving aerosol optical depth
445 over urban surfaces in MODIS dark target retrieval algorithm[J]. Atmos Meas Tech, 2016,
446 9(7): 3293-3308.
447 Hatzianastassiou, N. The direct effect of aerosols on the radiation budget and climate of the
448 Earth-atmosphere system: its variability in space and time. EGU General Assembly
449 Conference Abstracts EGU General Assembly Conference Abstracts, 2009.
450 He, J.; Zha, Y.; Zhang, J.; Gao, J.; Li, Y.; & Chen, X. (2015). Retrieval of aerosol optical
451 thickness from hj-1 ccd data based on modis-derived surface reflectance[J]. International
452 Journal of Remote Sensing, 2015, 36(3-4), 882-898.
453 Holben, B. N.; Tanré, D.; Smirnov, A. An emerging ground-based aerosol climatology: Aerosol

https://doi.org/10.5194/amt-2023-204
Preprint. Discussion started: 22 November 2023
© Author(s) 2023. CC BY 4.0 License.

Atmospheric Measurement Techniques Discussions

optical depth from AERONET[J]. J Geophys Res, 2001, 106, 12067-12097.

Hong, G.; Yang, P.; Gao, B. C.; Baum, B. A.; Hu, Y. X.; King, M. D. High cloud properties from three years of modis terra and aqua collection-4 data over the tropics. J Appl Meteorol Clim. 2007, 46(11): 1840-1856.

Huang X , Ding A .Aerosol as a critical factor causing forecast biases of air temperature in global numerical weather prediction models[J].Science Bulletin, 2021.DOI:10.1016/j.scib.2021.05.009.

Hsu, N. C.; Tsay, S. C.; King, M. D. Aerosol properties over bright-reflecting source regions[J]. IEEE Trans. Geosci. Remote Sens, 2004, 42(3):557- 569.

Kahn, Gaitley, B. J.; Martonchik, J.; Diner, D.; Crean, K. Misr global aerosol optical depth validation based on two years of coincident aeronet observations. J Geophys Res-atmos, 2005, 110.

Kahn, R. A.; Garay, M. J.; Nelson, D. L.; Yau, K. K.; Bull, M. A. Satellite-derived aerosol optical depth over dark water from MISR and MODIS: Comparisons with aeronet and implications for climatological studies. J. Geophys. Res. 2007, 112.

Kaufman, Yoram J. The MODIS 2.1-um channel--correlation with visible reflectance for use in remote sensing of aerosol.[J]. IEEE T Geosci Remote, 1997, 35, 1286-1298.

Kokhanovsky, A. A.; Curier, R. L.; Leeuw, G. D.; Grey, W. M. F. The intercomparison of AATSR dual-view aerosol optical thickness retrievals with results from various algorithms and instruments. Int. J. Remote Sens. 2009, 30 (17): 4525-4537.

Lee, S. S.; Donner L. J.; Penner J. E. Thunderstorm and stratocumulus: How does their contrasting morphology affect their interactions with aerosols?[J]. Atmos. Chem. Phys. 2010, 10(2), 6819-6837.

Li, E.; Zhang, Z.; Tan, Y. A Novel Cloud Detection Algorithm Based on Simplified Radiative Transfer Model for Aerosol Retrievals: Preliminary Result on Himawari-8 Over Eastern China[J]. IEEE T Geosci Remote, 2020, 59(3):1-12.

Li, Y.; Xue, Y.; Guang, J. Ground-Level PM2.5 Concentration Estimation from Satellite Data in the Beijing Area Using a Specific Particle Swarm Extinction Mass Conversion Algorithm[J].

https://doi.org/10.5194/amt-2023-204
Preprint. Discussion started: 22 November 2023
© Author(s) 2023. CC BY 4.0 License.

Remote Sens-basel, 2018, 10(12), 1906.

Li, Z.; Zhao, X.; Kahn, R.; Mishchenko, M.; Remer, L.; Lee, K. H. Uncertainties in satellite remote sensing of aerosols and impact on monitoring its long-term trend: a review and perspective. Ann. Geophys-germany, 2009, 27, 2755-2770.

Lu, S.; Xue, Y.; Yang, X.-H.; Leys, J.; Guang, J.; Che, Y.-H.; Fan, C.; Xie, Y.Q.; Li, Y. Joint Retrieval of Aerosol Optical Depth and Surface Reflflectance Over Land Using Geostationary Satellite Data. IEEE Trans. Geosci. Remote Sens. 2019, 57, 1489–1501.

Martonchik, J. V. Determination of aerosol optical denth and land surface directional reflectances using multiangle imagery. J. Geophys Res-atmos. 1997, 102 (D14): 17015-17022.

Martonchik, J. V.; Diner, D. J.; Crean, K. A.; Bull, M. A. Regional aerosol retrieval results from MISR. IEEE Trans. Geosci. Remote Sens. 2002, 40, 1520–1531.

Mironova, I. A. Aerosols over continental Portugal (1978-1993): their sources and an impact on the regional climate[J]. Atmos. Chem. Phys. 2015, 15(11):6407-6418.

Remer, L. A; Tanré, D.; Kaufman, Y. J. Algorithm for remote sensing of tropospheric aerosol from MODIS: Collection 005[J]. 2009.

Samset, B. H.; Sand, M.; Smith, C. J. Climate Impacts From a Removal of Anthropogenic Aerosol Emissions[J]. Geophys Res Lett, 2018, 45(2).

Sun, E.; Fu, C.; Yu, W. Variation and Driving Factor of Aerosol Optical Depth over the South China Sea from 1980 to 2020[J]. Atmosphere, 2022, 13, 372.

Sundstrom, A. M.; Kolmonen, P.; Sogacheva, L.; Leeuw, G. D. Aerosol retrieval over China with the AATSR dual view algorithm. Remote Sens. Environ. 2012, 116 (1): 189-198.

Wong, N.; Wong, S.; Lim, A.; Mcneil, D.; Huete, A. R. Impacts of spatial heterogeneity patterns on long-term trends of moderate resolution imaging spectroradiometer (modis) land surface temperature time series. J Appl Remote Sens. 2020, 14(1): 1.

Xie, Y.; Xue, Y.; Jie, G. Deriving a Global and Hourly Data Set of Aerosol Optical Depth Over Land Using Data From Four Geostationary Satellites: GOES-16, MSG-1, MSG-4, and Himawari-8[J].IEEE T Geosci Remote, 2019, 99:1-12.

Zhang, Y.; Li, Z.; Liu, Z. Retrieval of aerosol fine-mode fraction over China from satellite

https://doi.org/10.5194/amt-2023-204
Preprint. Discussion started: 22 November 2023
© Author(s) 2023. CC BY 4.0 License.

Atmospheric Measurement Techniques Discussions

510 multiangle polarized observations: validation and comparison[J]. Atmos Meas Tech, 2021, 2,

511 1655-1672.